Performance Evaluation of the NRCAN Wide Area System

S. Skone, M. E. Cannon
Department of Geomatics Engineering
University of Calgary

K. Lochhead, P. Héroux, F. Lahaye
Geodetic Survey Division, Natural Resources Canada

Biographies

Susan Skone is a Ph.D. student in the Department of Geomatics Engineering, The University of Calgary. She has B.Sc. degrees in math and physics (1989,1990), and an M.Sc. in space physics (1994), from the University of Alberta.

Dr. M.E. Cannon is a Professor in Geomatics Engineering at The University of Calgary. She has been involved with GPS research since 1984 and has published numerous papers on static and kinematic GPS positioning. She is the author of several GPS-related software programs.

Kim Lochhead graduated with a B.Sc. Eng. from The University of New Brunswick in 1977. He is currently working on applications related to the Canadian Active Control System.

Pierre Héroux graduated with a B.Sc. in Geodesy from Laval University in 1981. He has been involved in GPS projects for precise positioning and navigation in the private and public sectors for the past 15 years.

François Lahaye graduated with a B.Sc. in mathematics in 1987 and a M.Sc. in geodesy in 1991, both from Laval University, Québec. He has been involved in GPS projects dealing with orbit determination, precise positioning and navigation at the Geodetic Survey Division of NRCan since 1988.

Abstract

Since 1992, Geodetic Survey Division, Natural Resources Canada (NRCan) has been generating post-mission precise orbit and 30 second clock corrections using the Canadian Active Control System (CACS) as well as 22 additional International GPS Service for Geodynamics (IGS) global tracking stations. NRCan has undertaken a new initiative in which the precise orbits are predicted to facilitate real-time positioning. When accompanied with precise clock corrections, and the reformatting of data to be consistent with RTCM standards, users can obtain wide area positions which are automatically referenced to the national framework. In order to analyze the performance of the NRCan wide area system, several test were conducted on The University of Calgary test ranges. These tests include an analysis of the predicted orbit accuracy versus the post-mission orbit, a comparison of the wide area achievable accuracies, as well as a comparison of the wide area positions with those obtained from local area DGPS. Both static and kinematic tests were performed using various receiver technologies. In the case of the kinematic tests, an accurate reference trajectory was computed using carrier phase techniques in post-mission. The performance analysis includes measures of the accuracy of the system for each receiver tested, as well as the effects of latency.

1. Introduction

Since 1992, Geodetic survey Division, Natural Resources Canada (NRCan) has been generating post-mission precise orbit and 30-second clock corrections using the Canadian Active Control System (CACS), as well as 22 additional International GPS Service for Geodynamics (IGS) global tracking stations. These orbits have been demonstrated to be accurate to 10-20 cm while the clock corrections are accurate to the 1 ns level. Several tests have been conducted with this orbit and clock information [cf. *Lachapelle et al*., 1996] and several commercial software packages have incorporated their use for production work.

A desirable extension of the above initiative is to have access to the information in real-time. During the past year, NRCan has developed the capability to produce predicted orbits and rapid clock information that can be transmitted to users in real time. This information, combined with a single layer ionospheric grid, has formed the basis of a wide area system which can be used to generate ranging corrections. The objective of this paper is to assess the accuracy of these wide area corrections. In order to make this assessment, the predicted orbits and rapid clock corrections are analysed with respect to precise orbit and clock information. The wide area corrections are then applied to static and kinematic GPS data collected with a variety of single and dual frequency receiver types, and comparisons are made with GPS truth data. Comparisons with local area DGPS (LDGPS) are made to determine if the wide area system has the potential to replace such a system for some applications.

2. NRCan CACS Infrastructure

The Geodetic Survey Division of Geomatics Canada, in partnership with the Geological Survey of Canada, Natural Resources Canada, has been operating the CACS to provide improved GPS positioning capability in support of geodetic positioning, navigation and other spatial referencing applications. The system consists of a Canada-wide network of Active Control Points (ACP's), which track all GPS satellites. Presently, ACP's are located in Algonquin Park and Ottawa, Ontario, Yellowknife, Northwest Territories, Penticton, Victoria, Williams Lake and Holberg, British Columbia, St. John's, Newfoundland, Schefferville, Québec and Churchill, Manitoba (see Figure 1). Various communication technologies connect a Master Active Control System (MACS) with the ACP's. This CACS network configuration, augmented by about 22 globally distributed stations, provides continuous data for the determination of precise GPS satellites ephemerides, satellite clocks and earth orientation parameters. These CACS products

facilitate geodetic positioning at the 1-cm level and single point positioning at the 1-m level in post-processing, with several days delay.

In 1995-1996, the infrastructure necessary to collect the CACS tracking data at the MACS in real-time was put in place [*Caissy et al.*, 1996]. The real-time GPS component of the CACS (GPS·C) utilizes real-time tracking data along with the CACS high quality products to compute wide area GPS corrections in support of real-time applications.

3. Real-time GPS•C Concept

The term "wide area corrections" usually refers to the sum of corrections originating from GPS satellite orbits and clocks, and those corrections that account for delays experienced by the GPS signal as it travels through the troposphere and ionosphere. Since most individual correction terms have a predictable behavior over large geographic areas and variable time scales, it is more appropriate to model them separately. This approach is economical since it significantly reduces the number of GPS tracking stations necessary to facilitate a differential GPS service over a large territory.

The GPS·C implementation provides these "wide area corrections" to the users in real-time. The following sub-sections describe how the corrections are derived and then converted into range corrections.

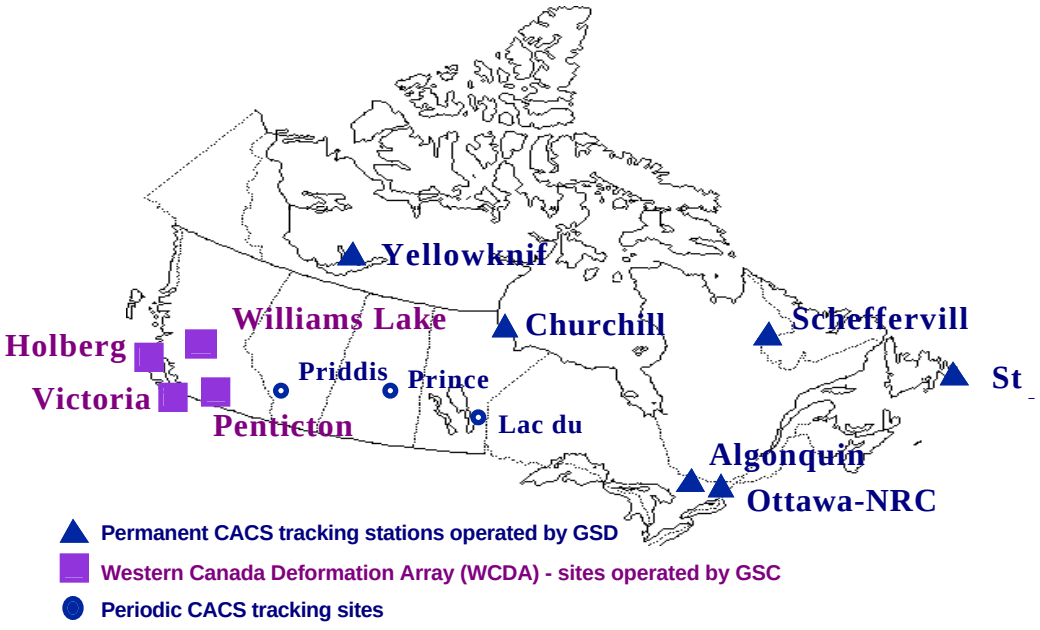

Figure 1. CACS network of automated tracking stations

3.1. Satellite orbit corrections

Improved satellite positions are provided through orbit prediction, based on the preceding 4 days of global dynamic solutions [*Tétreault et al.*, 1995], which are extrapolated up to 4 days ahead using a complete force model. The orbit predictions are updated every 24 hours. Typically, predictions for 12 to 60 hours are available in real-time. These orbits can then be compared with the broadcast ephemeris to produce orbital corrections.

3.2. Satellite clock corrections

The satellite clock corrections are derived from dual frequency tracking data collected in real-time from the ACP's. Ionosphere-free, carrier-phase smoothed pseudorange data for a given epoch, together with the available satellite orbit predictions and station coordinates, are used in a least squares adjustment to determine satellite and station clock corrections. Clock corrections determined in this manner are referred to as rapid clocks. One station clock is used as reference for the clock correction computations. When orbit predictions are not available for a satellite, the broadcast ephemeris is used. All computations are carried out in the NAD83 geodetic reference frame.

3.3. Ionospheric and tropospheric propagation delays

A simplified single-layer ionospheric model assumes that the ionosphere's total electron content (TEC) is concentrated in a thin spherical shell of variable electron density, located at an altitude of about 350 km above the earth's surface. The first order group delay for GPS signals propagating through the ionosphere is proportional to the total electron content along the signal paths and the inverse of the carrier frequency squared. The differences between ionospheric delays affecting the two GPS frequencies of 1575.42 (f_1) and 1227.6 MHz (f_2) are related to TEC in the following way:

$$d_{ion} = \tau_1 - \tau_2 = \frac{40.3\ TEC\ (f_1^{\,2} - f_2^{\,2})}{f_1^{\,2}\ f_2^{\,2}} \qquad (1)$$

where d_{ion} is in meters. The ionospheric delay d_{ion} is the inter-frequency difference between L1 and L2 pseudoranges ($\tau_2 - \tau_1$) and is the observation used to compute group delays. It must be free of receiver (d_r) and satellite (d_S) inter-frequency instrumental biases (Equation 2). These instrumental biases result from hardware delays in receiver and satellite L1 and L2 signal paths and can be estimated with ±0.5 nanosecond precision [*Gao et al.*, 1994].

$$I = d_{ion} - d_r - d_s \qquad (2)$$

An ionospheric pierce-point is located at the satellite-to-receiver signal path intersection with the single-layer. It is represented by the latitude (φ_{pp}), longitude/local solar time (λ_{pp}), and zenith angle(Z_{pp}). Bias-free ionospheric path delays can be mapped onto vertical delays I_v using the following function:

$$I_v = I\ \cos\left(Z_{pp}\right) \qquad (3)$$

The epoch vertical delays (I_v) between all network receivers and observed satellites serve to update a latitude versus longitude or latitude versus local solar time single layer ionospheric grid.

The tropospheric delay corrections are computed using either surface or standard meteorological data and a standard mapping function. It requires the input of receiver and satellite positions.

3.4. Range corrections derived from GPS•C

At times, it may be necessary to recombine GPS·C corrections for a specific location in order to determine satellite range corrections. This is the requirement of the RTCM-104 differential correction broadcast standard which was developed for GPS receivers located at DGPS reference stations [*RTCM*, 1994]. RTCM-104 range corrections can be generated for local reference stations from the wide area corrections, creating Virtual Active Control Points (VACP's) which need not be equipped with GPS receivers. The following paragraphs describe the VACP algorithms for localisation of wide area corrections.

The satellite orbit correction is the difference between broadcast and predicted satellite positions at the time of signal transmission. With both satellite positions available, the orbit correction is mapped onto the user range by computing differences between the two satellite-receiver ranges.

The satellite clock corrections are converted directly to satellite range corrections independent of receiver location. The satellite clock dithering introduced by Selective Availability makes this correction the largest in magnitude and rate of change.

The ionospheric corrections are usually represented by a grid of vertical delays for a single layer model, as in Section 3.3. Computation of the ionospheric correction requires the input of receiver and satellite positions to determine the latitude, longitude/solar time of the ionospheric pierce-point. With this information, the proper vertical delay may be extracted from the grid and mapped from the vertical onto the slant range using the computed zenith angle at pierce-point. The tropospheric correction is computed as per Section 3.3.

4. System Testing

4.1. Test and data description

Several tests were conducted at The University of Calgary test ranges to assess accuracies of both the wide area range corrections, and the position results generated using these corrections. A static point positioning test was conducted May 13 1996, using three different types of low cost single frequency receivers to independently determine position solutions: the Motorola VP Oncore (8-channel), the NovAtel GPSCard (Model 3951) (12-channel), and the Trimble Differential Survey Module (12-channel). This data was used in a comparison of position results generated using (1) precise clocks and precise orbits, (2) rapid clocks and predicted orbits, and (3) broadcast ephemerides with corresponding wide area corrections.

In addition to the three static receivers on May 13, three remote receivers, identical to the static monitor receivers, were operating in semi-kinematic mode. Observations from these receivers were used to generate position results using wide area corrections, for comparison with LDGPS solutions generated using corrections derived from monitor station observations. A 10 km precise kinematic trajectory was also computed and a comparison was made with position results generated using wide area corrections.

A static point positioning test was also conducted August 12 1996, in which observations were collected using two dual frequency receivers: the NovAtel MILLennium (24-channel), and the Trimble SSi (18-channel). Point positioning results were computed, using both dual frequency and wide area ionosphere corrections, in order to assess the relative accuracy of the two types of position solutions.

Note that wide area corrections derived for these tests were simulated as real-time measurements, and transformed into single range corrections, which were applied at 30s intervals in post-mission processsing. Prior to assessing the accuracy of position results generated in these tests, it is useful to first assess accuracies of the wide area corrections themselves.

4.2. Analysis of wide area corrections

4.2.1. Analysis of predicted orbits/rapid clocks

The wide area satellite orbit and clock correction terms are only as accurate as the predicted orbits and rapid clock corrections from which they are generated. An analysis of predicted orbits/rapid clocks therefore follows.

For the May and August system tests, real-time satellite clock corrections were generated in post-processing using data from nine CACS stations over the full 24 hours of each test day. The CACS stations ALBH, WILL, DRAO, YELL, CHUR, ALGO, NRC1, SCHE and STJO were used. Orbit predictions available on the test days, predicted 0 to 24 hours for the May data and 24 to 48 hours for the August data, were used in the generation of clock corrections.

The orbit predictions and satellite clock corrections were verified by comparison with final precise solutions from CACS. The precise orbits and clock corrections differ from the predicted values in that they are generated post-mission with a higher degree of accuracy. For comparison purposes in this paper, precise clocks and orbits are taken to be "truth". Figure 2 illustrates differences in the precise and predicted satellite coordinates for SV 2 on May 13 1996.

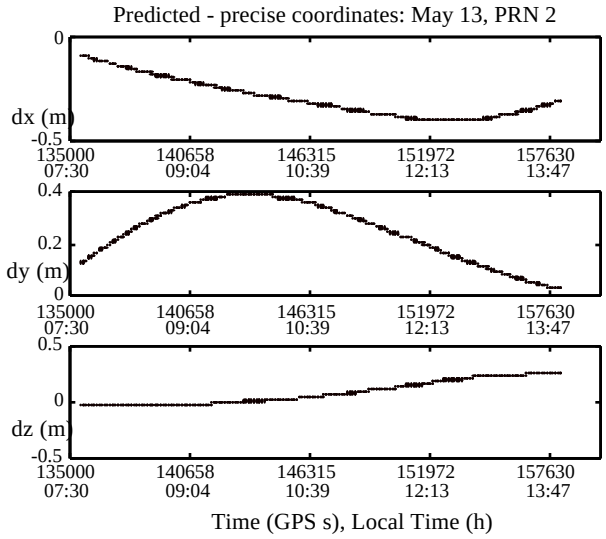

Figure 2. Comparison of precise and predicted orbital positions for PRN 2, May 13 1996. Cartesian coordinates are referred to NAD83.

For most satellites, three-dimensional rms values for orbital position differences were at the meter level after 24 hours and 3-5 meters after 48 hours.

Figure 3 shows the difference between rapid and precise clock corrections for SV 9 on May 13 1996. Such differences (on the order of 2-3 ns) are typical for all satellites.

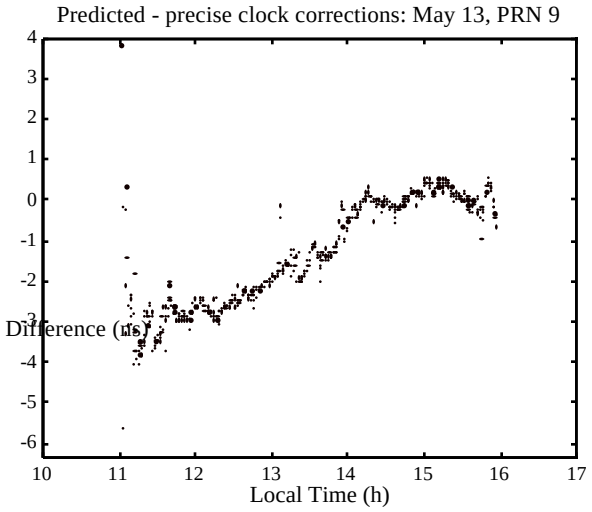

Figure 3. Comparison of precise and rapid clocks for PRN 9, May 13 1996.

4.2.2. Analysis of ionosphere grid versus observed ionospheric delays

A 3 × 3 degree grid of vertical ionospheric delays, based on the single-layer model, is estimated daily from dual-frequency observations collected by six to nine tracking stations of the CACS network. The grid covers a latitude band from 30 to 70 degrees north over a 24 hour period. The ionospheric grid quality is reflected by the level of agreement between vertical delays within individual cells over a 24 hour period. This agreement is 10-20 cm rms.

An independent means of assessing the quality of the single-layer grid is to compare modeled and observed ionospheric delays at stations that have not been included in the grid computation. For August 12, 1996, three CACS stations (WILL,SCHE,NRC1) were intentionally not included in the grid computation and direct comparisons were made between observed and modeled path delays for all satellites observed over the 24 hour period. The rms of differences were subsequently grouped per satellite PRN and elevation. Agreements of 30-50 cm rms for all satellites were obtained, with rms values ranging from approximately 10 cm at zenith to 1 m at the horizon. These results agree with those determined by *Kee* [1996] in an independent simulation of a wide area system.

4.3. Single frequency Results - May 13 1996

4.3.1. Static point positioning

The three different monitor receivers were placed at known positions on the roof of The University of Calgary Engineering building. A choke-ring was used only with the NovAtel antenna. Observations were collected for the period 133618 to 158429s GPS time and C/A code position solutions were computed, using a satellite elevation cutoff angle of ten degrees. Local tropospheric corrections were included in all static positioning results, as were wide area ionosphere corrections (interpolated from the wide area ionosphere grid). All static positioning results presented in this section are therefore consistent, for comparison purposes. The processing interval was 30s for all observations, and no carrier phase smoothing of the pseudorange observations was performed. Position solutions were computed using C^{3}NAVä , and a full description of this software is outlined in the operating manual [*Cannon et al.*, 1995]. The software and processing techniques are identical for all position results presented in this section.

In addition to the statistics presented in Section 4.2.1, it is useful to analyse how differences between predicted and precise orbits translate into position results. Tables 1 and 2 present position results obtained for the three receivers, using precise clocks and orbits (herein referred to as "precise products") and rapid clocks and predicted orbits (herein referred to as "predicted products"), respectively. Known reference coordinates for each receiver position have been subtracted from the relevant position solutions. Note that these tables and graphs have been calculated using the same set of observations for both the precise and predicted product results. Rapid clock corrections were sometimes unavailable for the same epochs as precise clock corrections, resulting in fewer satellite observations being included in predicted orbit position calculations and a degradation of the position solution for these epochs. It was therefore necessary to consider position results calculated using only those observations (for a given receiver) for which both precise and predicted product data were available, in order to make a consistent comparison of the relative accuracies of both solutions.

Table 1. Statistics for position results generated using precise clocks and orbits (N = sample size).

MEAN/RMS (m)

	LATITUDE	LONGITUDE	HEIGHT	N
NovAtel	0.336/0.570	0.097/0.348	-0.132/0.910	811
Trimble	0.161/1.091	0.090/0.808	-0.145/1.992	819
Motorola	-0.598/0.925	1.069/1.219	0.348/1.228	805

Table 2. Statistics for position results generated using rapid clocks and predicted orbits (N = sample size)

MEAN/RMS (m)

	LATITUDE	LONGITUDE	HEIGHT	N
NovAtel	0.283/0.739	-0.163/0.558	0.322/1.513	811
Trimble	0.106/1.141	-0.178/0.881	0.309/2.287	819
Motorola	-0.692/1.133	0.743/1.188	0.841/1.687	805

Rms values in Table 2 exceed those in Table 1 by as much as 60 cm (in the height component). Discrepancies between the position solutions in Tables 1 and 2 are attributed almost entirely to the differences between precise and rapid clock corrections.

Table 3 presents position results obtained using wide area corrections with the corresponding broadcast ephemerides. One set of wide area corrections was used for the three receivers, as generated for coordinates of the NovAtel receiver, which was located within 15 m of the other two receivers. These corrections were not transmitted real-time, such that latency effects are not included in the results. Additionally, the set of observations used to generate results in Tables 1 and 2 was also used to generate the results presented in Table 3, such that the three tables are consistent and comparable. Statistics for the wide area results are generally as good or better than rms values in Table 2, as one would expect (the wide area corrections being derived from rapid clocks and predicted orbits).

Table 3. Statistics for position results generated using broadcast ephemerides and the corresponding wide area corrections (N = sample size)

MEAN/RMS (m)

	LATITUDE	LONGITUDE	HEIGHT	N
NovAtel	0.145/0.536	0.047/0.417	-0.077/1.104	811
Trimble	-0.023/1.126	0.020/0.861	-0.069/2.119	819
Motorola	-0.843/1.244	0.979/1.218	0.365/1.443	805

In order to assess the effects of latency and present a more realistic set of statistics, latency effects were simulated and applied to the NovAtel position results in Table 3. These effects were simulated by modeling the range-error acceleration as a 4 mHz sinusoid (typical of that observed by *Kremer et al*. [1990]), initialized with random phase and an amplitude of 0.019 m/s^2. The results for latency intervals of 3.0s and 5.0s are shown in Table 4 for the NovAtel receiver.

Rms values increase by centimeters for a latency interval of 3.0s, and by 30 cm 3-d rms (1-σ) for a latency interval of 5.0s. Results in Table 4 are typical of those determined by *Kee* [1996] (1.5 to 4 m 3-d rms positioning accuracy for a 5-10s latency interval), although the 0.30 m increase in position error over Table 3 statistics is somewhat large. This results from using a worst case 0.019 m/s^2 upper bound range-error acceleration (σ = 0.01 m/s^2). Typical values of σ are often less than 0.005 m/s^2. The user can therefore expect results similar to, or better than, those presented in Table 4 for real-time applications of the wide area system.

Table 4. Revised statistics for NovAtel Table 3 results, with the addition of latency effects (for latency intervals = 3.0s, 5.0s)

MEAN/RMS (m)

INTERVAL	LATITUDE	LONGITUDE	HEIGHT
3.0s	0.154/0.547	0.048/0.466	-0.042/1.083
5.0s	0.158/0.702	0.048/0.576	-0.079/1.381

4.3.2. WADGPS versus LDGPS results

In this test, the three remote receivers were mounted on a vehicle, with the NovAtel antenna periodically placed at different sites for periods of static data collection.The surveyed coordinates of these sites are part of The University of Calgary test range, which was established using dual frequency Ashtech receivers. Network adjustment of the points yielded confidence regions of 0.13 m horizontally and 0.22 m vertically at a 95% confidence level [*Clarke*, 1995]. Nine such sites were used in this test, at distances between 16 km (site 1) and 96 km (site 9) from the monitor station. True positions of the Trimble and Motorola antennae at these various sites were determined using a semi-kinematic short baseline (typically <10 m) solution, where all ambiguities were resolved to integers, and standard deviations of the vector lengths were typically 0.50 m.

Code single difference position solutions were calculated for each period of static data collection at the various sites, for each receiver. These LDGPS solutions are compared with the relevant WADGPS single point solutions, as calculated using the broadcast ephemerides with corresponding wide area corrections. No carrier phase smoothing of the pseudoranges was performed for either the LDGPS or WADGPS solutions. Note that one set of wide area corrections was used to generate all WADGPS position results presented here. This set of corrections was generated using coordinates of the NovAtel receiver at the monitor station. A comparison of the LDGPS and WADGPS solutions for each receiver are shown in Figures 4, 5, and 6, where true positions have been subtracted from the relevant position calculations.

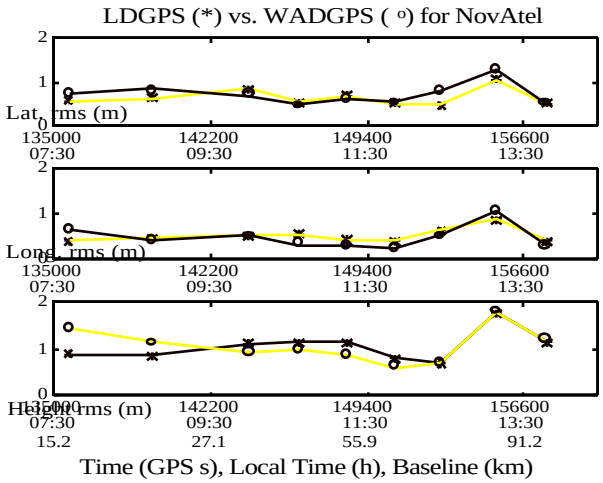

Figure 4. Comparison of LDGPS and WADGPS results for the NovAtel receiver

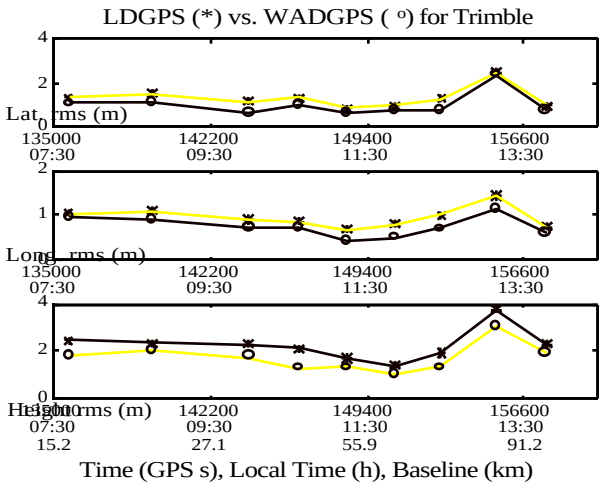

Figure 5. Comparison of LDGPS and WADGPS results for the Trimble receiver

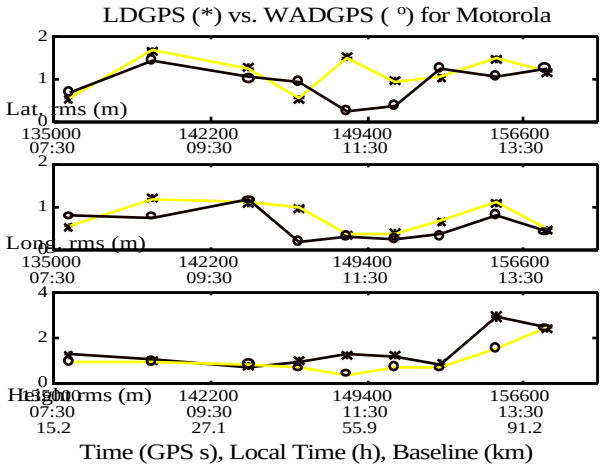

Figure 6. Comparison of LDGPS and WADGPS results for the Motorola receiver

Site occupation times were 2700s at the first site, and approximately 1200s at each of the remaining eight sites. Results are based on 30s data processing intervals and, similar to observations for the monitor stations, the observations for which no wide area corrections are available have been eliminated from the data set used to generate both sets of results. The LDGPS and WADGPS position results, for a given receiver, are therefore based on exactly the same set of observations.

LDGPS and WADGPS results are positively correlated for all three receivers. The larger rms values at site eight correspond to an increase in GDOP values, from 2.0 to 3.0, for all 3 receivers. Decorrelation between the two latitude solutions occurs at approximately 149000s for the Motorola receiver. This corresponds to an isolated interval in which the GDOP values are larger than 4.0 for the Motorola receiver and no solution was possible for several epochs. Table 5 presents the combined position statistics for all nine sites.

Table. 5. WADGPS versus LDGPS statistics (N = sample size)

a. Combined LDGPS Results: rms values (m)

	LATITUDE	LONGITUDE	HEIGHT	N
NovAtel	0.670	0.520	1.071	404
Trimble	1.396	0.995	2.355	404
Motorola	1.187	0.825	1.164	394

b. Combined WADGPS Results: rms values (m)

	LATITUDE	LONGITUDE	HEIGHT	N
NovAtel	0.762	0.553	1.168	404
Trimble	1.152	0.813	1.832	404
Motorola	0.967	0.658	1.144	394

4.3.3. Kinematic results

The kinematic test was conducted during the interval 137600 - 138300s GPS time, using the remote observations. The "true" kinematic trajectory was determined for each of the NovAtel and Trimble receivers using a carrier phase fixed integer ambiguity solution (σ = 0.05m). The ambiguities were fixed during a 2700s static initialization period at the first site of the test range, for a baseline of approximately 16 km. It was not possible to fix the Motorola ambiguities to integers during this static initialization period, since less than four satellites were tracked by the Motorola for part of this interval, and no kinematic trajectory was obtained for the Motorola receiver.

The kinematic trajectory was 10 km long and directed approximately east to west, with a height profile in the range 1175-1275 m. The vehicle's speed during the interval of kinematic observations was approximately 50 km/h. Position solutions were calculated for the NovAtel and Trimble receivers, using remote observations and the wide area corrections generated for coordinates of the NovAtel monitor station.

Differences between wide area position solutions and the true kinematic trajectory are shown in Figure 7.

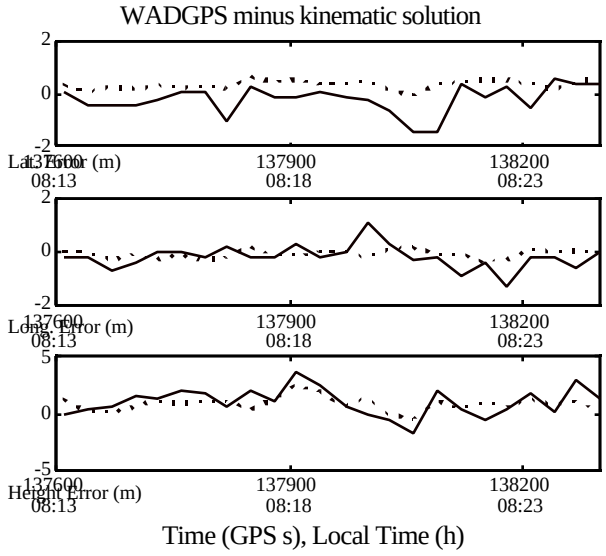

Figure 7. WADGPS vs. kinematic position results for the NovAtel (dashed line) and Trimble receivers

Table 6 presents position statistics, as calculated for the entire interval of kinematic data. These statistics are similar to those values for static WADGPS position results in Table 5, and confirm the validity of using the wide area corrections in a dynamic environment.

Table 6. Statistics for the position differences in Figure 7 (N = sample size)

RMS values (m)

	LATITUDE	LONGITUDE	HEIGHT	N
NovAtel	0.393	0.422	1.300	23
Trimble	0.525	0.507	1.644	23

5. Dual Frequency Results - August 12 1996

5.1. Static point positioning

This point positioning test was similar to that conducted on May 13 1996. The NovAtel and Trimble dual frequency receivers were located at known positions on the roof of The University of Calgary Engineering building , and observations were collected for the period 158000 - 162000s GPS time. C/A code position solutions were computed using either full wide area corrections, or wide area clock and orbit corrections in combination with dual frequency estimates of the ionosphere. Localised troposphere corrections were also included in both types of position solutions. Processing of this data was identical to the processing described in Section 4.3.1.

Figure 8 illustrates height position results for the NovAtel receiver, as calculated using wide area corrections with the broadcast ephemeris. Figure 8 also illustrates position results calculated using wide area clock, orbit and troposphere corrections, combined with dual frequency estimates of the ionospheric delay. The dual frequency ionosphere corrections have been corrected for satellite L1-L2 interchannel biases, using the broadcast group delay Tgd.

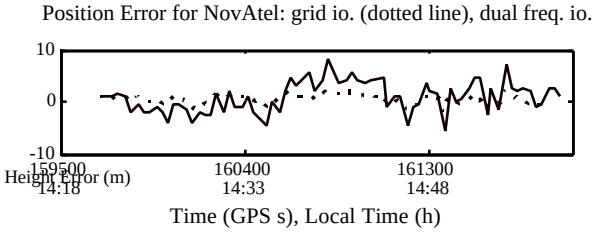

Figure 8. Height results for the NovAtel receiver, using wide area ionosphere corrections (dashed line), and dual frequency ionosphere corrections

Position results (in all components) generated using the dual frequency ionosphere values are significantly noisier than those position results generated using wide area ionosphere corrections. Table 7 presents statistics which quantify the the larger rms values in Figure 8. Only the Trimble latitude rms is improved in Table 7b, over the results in Table 7a.

Table 7. Statistics for position results generated using (a) wide area ionosphere corrections, and (b) dual frequency ionosphere corrections

a. Wide area ionosphere corrections
MEAN/RMS (m)

	LATITUDE	LONGITUDE	HEIGHT	N
NovAtel	-0.430/1.001	0.836/1.584	0.435/1.010	113
Trimble	-0.974/1.061	0.871/0.919	-0.071/1.456	113

b. Dual frequency ionosphere corrections:
MEAN/RMS (m)

	LATITUDE	LONGITUDE	HEIGHT	N
NovAtel	-0.211/1.140	1.032/2.010	0.684/2.300	113
Trimble	-0.109/0.422	.775/1.096	1.200/1.720	113

Larger rms values in Table 7b result directly from the additional L2 noise, introduced into the position solution by application of the dual frequency ionosphere corrections. Carrier smoothing of the L1 pseudoranges, after applying ionosphere corrections, does not improve the position results in Table 7b significantly.

Figure 9 shows the dual frequency ionosphere delay (calculated for both the NovAtel and Trimble receivers), as compared with the wide area ionosphere corrections, for SV 26.

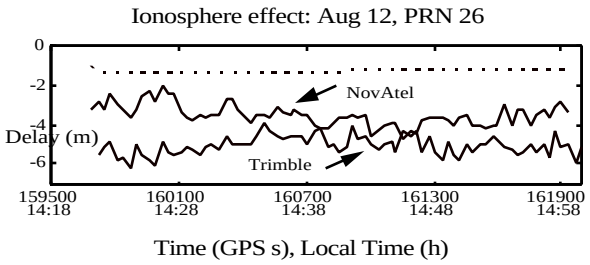

Figure 9. Comparison of dual frequency ionosphere delay values with wide area ionosphere corrections (dashed line).

Note that theoretical values of ionosphere delay are always positive. Negative values in Figure 9 result from hardware delays between the satellite Ll and L2 channels (in addition to the broadcast group delay Tgd) and receiver L1-L2 interchannel biases. If the negative offset is attributed to receiver interchannel biases, as it is for the wide area corrections, the bias is absorbed into estimates of the receiver clock errors, and eliminated, during position processing.

Raw estimates of the dual frequency ionosphere effect do not apear to improve position results, over those calculated using wide area ionosphere corrections. Smoothing of the raw dual frequency values of ionospheric delay will improve the position results, by removing excess L2 noise. Preliminary tests using such processing techniques suggest that, once the excess noise has been removed through smoothing, positioning accuracies are on the order of those results generated using the wide area ionosphere corrections, and are consistent with those generated using single frequency receivers (Section 4.3).

It must be noted that there was a low level of ionospheric activity on this day, there being very little reconnection at the dayside magnetosphere, as reflected in low values of the Z_{gsm} component of the interplanetary magnetic field (measured by the WIND satellite). Estimates of the dual frequency ionospheric delay may therefore degrade position solutions, through increased noise, without improving absolute position accuracies significantly. Further testing of position results generated using dual frequency ionosphere corrections is necessary, under a variety of ionospheric conditions, in order to determine the relative accuracy of position results generated using dual frequency estimates of the ionospheric delay, versus those generated using wide area ionosphere corrections.

6. Conclusions

Once the GPS· C system is operational, users will be able to obtain GPS corrections in the RTCM format at any point in Canada and perform single point positioning automatically referenced to the national geodetic framework. In this paper, positioning accuracies using the wide area corrections were consistently less than 3 m (3-d rms, 1-σ), and often less than 2 m, for both static and kinematic positioning tests of the system. Rms errors were generally largest in the height component. These results are in agreement with the results of a WADGPS simulation published by *Kee* [1996], where WADGPS positioning errors were approximately 2 m (3-d rms) for a system of twelve monitor stations across the continental United States. Such results indicate an improvement of 98-99% accuracy over single frequency stand-alone positioning errors. Test results presented in this paper were also consistent for various receiver technologies, and are not expected to degrade significantly for real-time applications, in which latency effects become an additional source of error. Discussions of projected real-time positioning accuracies are only speculative, however, and further tests are necessary to verify the simulated real-time results presented here.

Predicted and precise orbital positions were found to differ by one meter after a 24 hour prediction period, and by 3-5 meters after a 48 hour prediction period, while rapid and precise clock corrections were found to differ by a few ns. The wide area clock and orbit corrections are derived from these predicted orbits and rapid clocks, with accuracies dependent on the agreement of predicted orbits and rapid clocks with the precise values. Ionospheric grid values were found to have accuracies of 30-50 cm rms.

The positioning accuracies of single frequency receivers, operating in both static and kinematic modes, are on the order of 1.5-3 m (3-d rms, 1-σ), depending on receiver type, the highest accuracies being achieved with the NovAtel GPSCard (1.5 m 3-d rms). Note that higher static point positioning accuracies for the NovAtel receiver may have resulted from using a choke-ring with the NovAtel antenna during testing. These results are comparable with those position results generated for dual frequency receivers (using wide area ionosphere corrections), and are encouraging (single frequency units being lower-cost, ranging from a few hundred to several thousand dollars). Additionally, the single frequency WADGPS position results were in agreement, and were generally slightly better, than position results generated using LDGPS. The WADGPS solutions did not appear to degrade significantly with increased distance (up to 96 km) from the coordinates for which the wide area corrections were generated, even though the level of ionospheric activity during this testing period (May 13 1996) was unsettled to active, as reflected in the planetary Kp indices at College, Alaska and Fredericksburg, Virginia (which ranged from 2 to 4).

Static point positioning results for the dual frequency receivers, as generated using wide area corrections, had accuracies on the order of 2 m (3-d rms, 1-σ), which agree with the position results determined for single frequency receivers. Positioning accuracies were not improved by using dual frequency ionosphere corrections in place of the wide area ionosphere corrections, the dual frequency results having accuracies of approximately 2.5-3 m (3-d rms, 1-σ). These results may be improved upon by

smoothing the raw values of dual frequency ionosphere delay. Further tests are necessary, however, under a variety of ionospheric conditions, to determine the relative accuracy of wide area ionosphere corrections versus dual frequency estimates of ionospheric delay, for a given receiver.

7. Acknowledgements

The authors thank Jim Stephen and Jamie Henriksen for data collection and preprocessing. One of us (S.S.) acknowledges support from the Natural Sciences and Engineering Research Council of Canada (NSERC).

8. References

Caissy, M., P. Héroux, F. Lahaye, K MacLeod, J. Popelar, J. Blore, D. Decker and R. Fong (1996), "Real-Time GPS Corrections Service of the Canadian Active Control System", *ION GPS-96 Proceedings*, September, 1996.

Cannon, M.E., G. Lachapelle, and W. Qui (1995), "C^{3}NAVä Operating Manual", Version 2.0, The University of Calgary, Calgary, Alberta.

Clarke, C. (1995), "Report on the Static GPS Survey of the Springbank to Drayton Valley Baseline."

Duval, R., P. Héroux and N. Beck (1996), "Canadian Active Control System - Delivering the Canadian Spatial reference System", *GIS'96 Conference Proceedings (CD-ROM file C2-4)*, Fort Collins, Col., U.S.A.: GIS World Inc.

Gao, Y., P. Héroux and J. Kouba (1994), "Estimation of GPS Receiver and Satellite L1/L2 Signal Delay Biases Using Data from CACS", *Proceedings of the International Symposium on Kinematic Systems in Geodesy, Geomatics and Navigation*, Banff, Canada, August 30-September 2, pp. 109-117.

Kee, C. (1996), "Wide Area Differential GPS", *Global Positioning System: Theory and Applications, vol 2,* 1st ed., American Institute of Aeronautics Inc., ch. 3, pp 81-115.

Kremer, T.K., R. M. Kalafus, P.V.W. Loomis, and J.C. Reynolds (1990), "The Effect of Selective Availability on Differential GPS Corrections", *Navigation*, vol. 37, pp 39-52.

Lachapelle, G., M.E. Cannon, W. Qui, and C. Varner (1996), "Precise Aircraft Single Point Positioning Using Post-Mission Orbits and Satellite Clock Corrections", *Journal of Geodesy*, vol. 70, pp 562-571.

RTCM (1994), "Recommended Standards for Differential Navstar GPS Service", Version 2.1, RTCM SC-104, Washington, D.C.

Tétreault, P., J. Kouba, R. Ferland and J. Popelar (1995), "NRCan (EMR) Analysis Report", in "1994 IGS Annual Report, International", GPS Service for Geodynamics, IGS Central Bureau at Jet Propulsion Laboratory, pp. 213-232.